Journal of Engineering Mathematics (2005) 53: 79–98
DOI 10.1007/s10665-005-4752-7

A comparison of stability and bifurcation criteria for a compressible elastic cube

D.M. HAUGHTON
Department of Mathematics, University of Glasgow, University Gardens, Glasgow G12 8QW, UK (dmh@maths.gla.ac.uk)

Received 28 June 2004; accepted in revised form 31 March 2005

Abstract. A version of Rivlin's cube problem is considered for compressible materials. The cube is stretched along one axis by a fixed amount and then subjected to equal tensile loads along the other two axes. A number of general results are found. Because of the homogeneous trivial and non-trivial deformations exact bifurcation results can be found and an exact stability analysis through the second variation of the energy can be performed. This problem is then used to compare results obtained using more general methods. Firstly, results are obtained for a more general bifurcation analysis. Secondly, the exact stability results are compared with stability results obtained via a new method that is applicable to inhomogeneous problems. This new stability method allows a full nonlinear stability analysis of inhomogeneous deformations of arbitrary, compressible or incompressible, hyperelastic materials. The second variation condition expressed as an integral involving two arbitrary perturbations is replaced with an equivalent nonlinear third order system of ordinary differential equations. The positive definiteness condition is thereby reduced to the simple numerical evaluation of zeros of a well behaved function.

Key words: bifurcation, nonlinear elasticity, stability

1. Introduction

The purpose of this paper is twofold. Firstly, we investigate one version of Rivlin's cube problem [1, 2] for compressible materials. In the course of this investigation we look at the relationship between the bifurcation criterion and the stability criterion. The actual problem that we consider is the case of equi-biaxial loading of a cube. All deformations are assumed to be homogeneous and the simplicity of the problem allows us to make considerable analytic progress.

The corresponding problems for incompressible materials have been considered by several authors. Results for the bifurcation problem have been given by Wu and Widera [3] for Mooney–Rivlin materials (which are equivalent to Neo-Hookean materials for this problem). More general bifurcation results are given by Sawyers and Rivlin [4]. Additional results and a review can be found in [5, 6]. For stability of both the trivial and non-trivial solutions we require that the second variation of the total energy be positive. See [7] and [8] for the formulation of this problem and some general results. The stability problem for an incompressible cube has been considered by Sawyers and Rivlin [9] where the cube was assumed to be composed of Neo-Hookean material. Because of the homogeneous deformation it is possible to factorise the argument of the second variation and so stability results follow in a straightforward way.

For the compressible problem considered here Ogden [10] has given some general results and also results for specific strain-energy functions. We show in general that the trivial and

non-trivial solution, should one exist, are perpendicular when plotted in the plane of the principal stretches. Also, bifurcation points occur at and only at turning points of the non-trivial loading and all bifurcation points are neutrally stable. Rivlin and Beatty [11] have recently looked at the full cube problem for compressible materials.

In a recent paper Chen and Haughton [12] have developed a method to study the full nonlinear stability of inhomogeneous deformations based on the second variation of the energy. The method is quite general and can deal with full three-dimensional problems [13]. The method involves the solution of a nonlinear system of ordinary differential equations for $y_i(x)$, say, where the range of the subscript i depends on the dimension of the problem. Stability is ultimately determined by the positive definiteness of a simple matrix based on y_i evaluated at one end of the domain. For two-dimensional problems, such as the one we consider here, we have a third-order system. For a three-dimensional problem we need a sixth order system. In contrast the corresponding bifurcation criterion for two-dimensional problems involves the solution of a linear fourth-order system (and a linear sixth-order system for a three-dimensional problem).

Our second aim in this paper is to apply the method proposed by Chen and Haughton [12] with a view to comparing results with both bifurcation and stability results obtained more directly. By adjusting parameters in the problem a wide variety of different types of bifurcation behaviour can be investigated. We can also look at problems where there is a loss of ellipticity. For the inhomogeneous problems investigated using the method of Chen and Haughton [12], Haughton and Kirkinis [13, 14] the matrix determining stability has always become negative semi-definite through the determinant becoming zero. By considering different types of bifurcation mode we investigate the possibility of other methods of loosing positive definiteness.

2. Basic equations

We consider the homogeneous deformation of a compressible elastic cube

$$0 \leq X \leq A, \quad 0 \leq Y \leq A, \quad 0 \leq Z \leq A, \tag{1}$$

where (X, Y, Z) are the material cartesian coordinates. The body is composed of a homogeneous, isotropic, compressible elastic material in the reference configuration. It is assumed to undergo the homogeneous deformation

$$x = \lambda_1 X, \quad y = \lambda_2 Y, \quad z = \lambda_3 Z, \tag{2}$$

where (x, y, z) are the spatial cartesian coordinates, and λ_i, $i = 1, 2, 3$ are the constant, positive, principal stretches. The deformed cube then occupies the region

$$0 \leq x \leq b = \lambda_1 A, \quad 0 \leq y \leq a = \lambda_2 A, \quad 0 \leq z \leq \lambda_3 A. \tag{3}$$

We suppose that the deformation is accomplished by equi-biaxial dead loads T applied to the sides $X = 0, A$ and $Y = 0, A$ with the remaining sides $Z = 0, A$ held a fixed distance apart. The axial stretch λ_3 can then be regarded as a prescribed parameter for this problem. The equilibrium equations are automatically satisfied for this homogeneous deformation and the dead loading T is given by

$$T = W_1 = W_2, \tag{4}$$

where $W(\lambda_1, \lambda_2, \lambda_3)$ is the strain-energy function of the material and subscripts indicate partial differentiation, $W_i = \partial W/\partial \lambda_i$. Since the material is assumed to be isotropic W is symmetric in its arguments. The second equation in (4) then gives either

$$\lambda_1 = \lambda_2, \tag{5}$$

which we shall refer to as the trivial solution, or,

$$W_1 = W_2, \quad \lambda_1 \neq \lambda_2. \tag{6}$$

Taking the limit as $\lambda_2 \to \lambda_1 = \lambda$, say, in (6), and using the symmetry of W in λ_1 and λ_2, we obtain the bifurcation point where the trivial and non-trivial solutions cross. This is given by

$$W_{11}(\lambda, \lambda, \lambda_3) = W_{12}(\lambda, \lambda, \lambda_3). \tag{7}$$

The non-trivial solution (6) can be regarded as an implicit equation for $\lambda_2(\lambda_1)$. Using this interpretation and differentiating with respect to λ_1 we have

$$\frac{\mathrm{d}\lambda_2}{\mathrm{d}\lambda_1} = \frac{W_{11} - W_{12}}{W_{22} - W_{12}}. \tag{8}$$

If we look at the limiting case $\lambda_2 \to \lambda_1 = \lambda$, by using $(4)_2$, l'Hôspital's rule and the symmetry of W in λ_1 and λ_2 we have

$$\left.\frac{\mathrm{d}\lambda_2}{\mathrm{d}\lambda_1}\right|_{\lambda_1=\lambda_2=\lambda} = \pm 1, \tag{9}$$

for all materials and any λ_3. Clearly $\mathrm{d}\lambda_2/\mathrm{d}\lambda_1 = 1$ corresponds to the gradient along the trivial solution ($\lambda_1 = \lambda_2$) and $\mathrm{d}\lambda_2/\mathrm{d}\lambda_1 = -1$ to the non-trivial (post bifurcation) solution, should one exist. Hence at a bifurcation point the trivial and non-trivial solutions are perpendicular in the (λ_1, λ_2) plane. Also, from $(4)_1$,

$$\frac{\mathrm{d}T}{\mathrm{d}\lambda_1} = W_{11} + W_{12}\frac{\mathrm{d}\lambda_2}{\mathrm{d}\lambda_1} = \frac{W_{11}W_{22} - W_{12}^2}{W_{22} - W_{12}}. \tag{10}$$

Taking the limit as $\lambda_2 \to \lambda_1 = \lambda$ along the non-trivial solution path we have

$$\left.\frac{\mathrm{d}T}{\mathrm{d}\lambda_1}\right|_{\lambda_1=\lambda_2=\lambda} = W_{11}(\lambda, \lambda, \lambda_3) - W_{12}(\lambda, \lambda, \lambda_3). \tag{11}$$

Hence, by comparing (7) with (11), we see that if a bifurcation point exists (and it may not for some combinations of material parameters and stretch λ_3) then it must occur at a stationary point of the non-trivial loading where T is regarded as a function of λ_1. That is, a stationary point of the non-trivial solution path.

We also note that if we consider the loading along the trivial path $\lambda_1 = \lambda_2 = \lambda$, say, then (4) gives

$$\frac{\mathrm{d}T}{\mathrm{d}\lambda} = W_{11}(\lambda, \lambda, \lambda_3) + W_{12}(\lambda, \lambda, \lambda_3). \tag{12}$$

3. Formal bifurcation analysis

For completeness we give a very brief description of the incremental equations that can be found in [5], for example. We then show how the bifurcation criterion (7) is recovered. In the absence of body forces the incremental equilibrium equations can be written

$$\operatorname{div} \dot{\mathbf{s}}_o = \mathbf{0}, \tag{13}$$

where div is the divergence operator in the current configuration and $\dot{\mathbf{s}}_o$ is the increment in the nominal stress evaluated in the current configuration. The incremental surface loading is given by

$$\dot{\mathbf{s}}_o^T \mathbf{n}, \tag{14}$$

where $\mathbf{n}$ is the unit outward normal to the surfaces. The incremental constitutive law is

$$\dot{\mathbf{s}}_o = \mathbf{B}\boldsymbol{\eta}^T, \tag{15}$$

where $\mathbf{B}$ is the fourth-order tensor of instantaneous moduli in the current configuration, $\mathbf{I}$ is the identity and we have written $\boldsymbol{\eta}$ for $\dot{\mathbf{F}}_o$, where $\mathbf{F}$ is the deformation gradient. The non-zero components of $\mathbf{B}$, given in [5, p. 343] in a different notation, are

$$\left.\begin{aligned} B_{iijj} = B_{jjii} &= \frac{\lambda_i \lambda_j}{J} \frac{\partial^2 W}{\partial \lambda_i \partial \lambda_j}, \\ B_{ijij} &= \lambda_i^2 \frac{\sigma_i - \sigma_j}{{\lambda_i}^2 - {\lambda_j}^2}, \quad i \neq j, \ \ \lambda_i \neq \lambda_j, \\ B_{ijij} &= (B_{iiii} - B_{iijj} + \sigma_i)/2, \quad i \neq j, \ \ \lambda_i = \lambda_j, \\ B_{ijij} - B_{ijji} &= B_{ijij} - B_{jiij} = \sigma_i, \quad i \neq j, \end{aligned}\right\} \tag{16}$$

where

$$\sigma_i = \frac{\lambda_i}{J} \frac{\partial W}{\partial \lambda_i}, \quad J = \lambda_1 \lambda_2 \lambda_3, \tag{17}$$

are the principal values of the Cauchy stress tensor. We shall assume that the Baker-Ericksen inequalities hold [15, p. 158] so that $B_{ijij} > 0$, for $i \neq j$. The cube is subjected to an incremental displacement of the form

$$\dot{\mathbf{x}}_o = (u(x, y), v(x, y), 0), \tag{18}$$

with respect to Cartesian coordinates. Hence $\boldsymbol{\eta}$ has components

$$\boldsymbol{\eta} = \begin{bmatrix} u_x & u_y & 0 \\ v_x & v_y & 0 \\ 0 & 0 & 0 \end{bmatrix}, \tag{19}$$

where subscripts denote partial derivatives.

We suppose that there is no incremental displacement normal to the surfaces $y = 0, a$ and that there is no incremental shear stress on these surfaces. From (14), (15) and (16) we then have

$$v = 0, \ \ u_y = 0, \ \ y = 0, a. \tag{20}$$

The incremental loading on the surfaces $X = 0, A$ is taken to be zero so that

$$\dot{\mathbf{s}}_o^T \mathbf{n} = \mathbf{0}, \quad x = 0, b, \tag{21}$$

where we recall that $b=\lambda_1 A$. We look for separable solutions and write

$$u=f_n(x)\cos\left(\frac{n\pi y}{a}\right), \qquad v=g_n(x)\sin\left(\frac{n\pi y}{a}\right), \tag{22}$$

where there is implied summation $n=0\ldots\infty$. Substituting (19) with (22), (16) and (17) in (13) we obtain

$$B_{1111}\frac{\mathrm{d}^2}{\mathrm{d}x^2}f(x)-B_{2121}\alpha^2 f(x)-\alpha\,(B_{1122}+B_{1221})\frac{\mathrm{d}}{\mathrm{d}x}g(x)=0, \tag{23}$$

and

$$\alpha\,(B_{1122}+B_{1221})\frac{\mathrm{d}}{\mathrm{d}x}f(x)-B_{1212}\frac{\mathrm{d}^2}{\mathrm{d}x^2}g(x)+B_{2222}\alpha^2 g(x)=0, \tag{24}$$

where

$$\alpha=\frac{n\pi}{a}. \tag{25}$$

We shall continue by assuming that we are on the trivial solution ($\lambda_1=\lambda_2$) as this affords some simplification. The problem for the non-trivial solution follows in a very similar but more complicated way. Eliminating $g(x)$ between (23) and (24) we obtain the single equation

$$\frac{\mathrm{d}^4}{\mathrm{d}x^4}f(x)-2\alpha^2\frac{\mathrm{d}^2}{\mathrm{d}x^2}f(x)+\alpha^4 f(x)=0, \tag{26}$$

where we have used (16) and made the assumption that $B_{1111}\neq 0$ and $B_{1122}+B_{1221}\neq 0$. These special cases are considered below. Equation (26) can be solved and we write the solution as

$$f(x)=C_1\cosh(\alpha x)+C_2\sinh(\alpha x)+C_3 x\cosh(\alpha x)+C_4 x\sinh(\alpha x), \tag{27}$$

where C_i, $i=1,\ldots,4$ are constants.

The four remaining boundary conditions (21) can be written

$$\begin{aligned}&B_{1122}B_{1212}B_{1111}f'''+(B_{1122}{}^3-(B_{1122}+B_{1221})B_{1111}{}^2+2B_{1122}{}^2B_{1221}\\&\quad-(B_{1212}-B_{1221})(B_{1212}+B_{1221})B_{1122})\alpha^2 f'=0,\\&B_{1212}B_{1111}f''+\alpha^2(B_{1221}{}^2-B_{1212}{}^2+B_{1122}B_{1221})f=0, \quad x=0,\,b.\end{aligned} \tag{28}$$

Since we are on the trivial solution $b=a$.

If we now substitute the solution (27) in the four boundary conditions (28) we have four homogeneous equations for the four constants of integration C_i, $i=1,\ldots,4$. The bifurcation criteria is that there exists a non-trivial solution to these equations. This leads to the requirement that a 4×4 determinant should vanish. After some manipulation the bifurcation criteria can be factorised and we require that

$$\begin{aligned}(B_{1111}-B_{1122})^2 B_{1111}^2\Big\{&(B_{1111}^2-B_{1122}^2+3B_{1111}\sigma_1+B_{1122}\sigma_1)^2(\cosh^2(n\pi)-1)\\&-(B_{1111}-B_{1122})^2(B_{1111}+B_{1122}-\sigma_1)^2 n^2\pi^2\Big\}B_{1212}^2=0,\end{aligned} \tag{29}$$

along the trivial solution path ($b=a$). An equivalent but rather longer equation is found for the non-trivial path in a straightforward way. There are two possible bifurcation modes since $B_{1212}>0$ from the Baker-Ericksen inequalities and we have assumed for the moment that

$B_{1111} \neq 0$. Clearly we recover the homogeneous bifurcation criterion (7) and one other possibility. This second possibility,

$$(B_{1111}^2 - B_{1122}^2 + 3\,B_{1111}\,\sigma_1 + B_{1122}\,\sigma_1)^2(\cosh^2(n\pi) - 1) - (B_{1111} - B_{1122})^2\,(B_{1111} + B_{1122} - \sigma_1)^2\,n^2\pi^2 = 0\,, \tag{30}$$

reflects the more general character of the bifurcation analysis where the post-bifurcation is arbitrary rather than being constrained to be homogeneous. This particular mode does not feature in our calculations presented below.

There are two special cases, if $B_{1111} = 0$ for some value of λ then it is easily shown that g is arbitrary apart from the requirement that both g and g' satisfy zero boundary conditions. In this special case we also have $f = g'/\alpha$ and so the boundaries do not move and the square shape is retained. The deformation does however become inhomogeneous and so we have a form of "internal" bifurcation. We note that the condition

$$B_{iiii} > 0\,, \tag{31}$$

is a necessary condition for strong ellipticity, see Ogden [5, p. 416], for example.

If $B_{1122} + B_{1221} = 0$ then we do not get such a simple solution for $f(x)$. Eventually we arrive at the bifurcation criterion (7) again so there is nothing new.

To illustrate possible behaviour we consider simple "single-term" strain-energy functions of the form

$$W(\lambda_1, \lambda_2, \lambda_3) = 2\,\mu\,\left\{\lambda_1{}^m + \lambda_2{}^m + \lambda_3{}^m + \beta\,(J-1)^2 - m\,(J-1) - 3\right\}/m^2\,, \tag{32}$$

where μ is the positive ground state shear modulus, $m \neq 0$, not necessarily an integer, is a material parameter and β can be written

$$\beta = m\,(3\,\kappa\,m - 2\,m\mu + 6\,\mu)/12\mu\,, \tag{33}$$

in terms of the bulk modulus κ. This class of materials is chosen simply to illustrate different types of behaviour. Mathematically this is convenient but they are not necessarily a good choice for actual material modelling. For such materials the equilibrium equation ($W_1 = W_2$) can be written

$$6\,(\lambda_1{}^{m-1} - \lambda_2{}^{m-1}) - (\lambda_1 - \lambda_2)\,\lambda_3\,(2\,m - 12 - 3\,\bar{\kappa}\,m + J\,(3\,\bar{\kappa}\,m - 2\,m + 6)) = 0\,, \tag{34}$$

where $\bar{\kappa} = \kappa/\mu$. Clearly, $\lambda_1 = \lambda_2$ is the trivial solution and, depending on the material parameters and the stretch λ_3, there may be other solutions $\lambda_2(\lambda_1)$, at least for some range of values of λ_1.

If we take $J \equiv 1$ in (32) we have a class of single-term incompressible materials. Ogden [5] has shown that, for these incompressible materials, $m = 1$ is a special case and typical post-bifurcation behaviour is different depending on $m > 1$ or $m < 1$. The situation is rather more complicated for compressible materials due to the extra parameter κ. It turns out that $m = 1$ in (32) is a special case. However, we can construct other compressible strain-energy functions that reduce to the same incompressible materials when $J \equiv 1$ where $m = 1$ does not show any particularly special features. One such strain-energy function is given by

$$W(\lambda_1, \lambda_2, \lambda_3) = 2\,\mu\,\left\{\lambda_1{}^m + \lambda_2^m + \lambda_3{}^m + \beta\,\log(J) - (m+\beta)\,(J-1) - 3\right\}/m^2\,, \tag{35}$$

with

$$\beta = m\,(2\,m\mu - 3\,\kappa\,m - 6\,\mu)/6\,\mu\,. \tag{36}$$

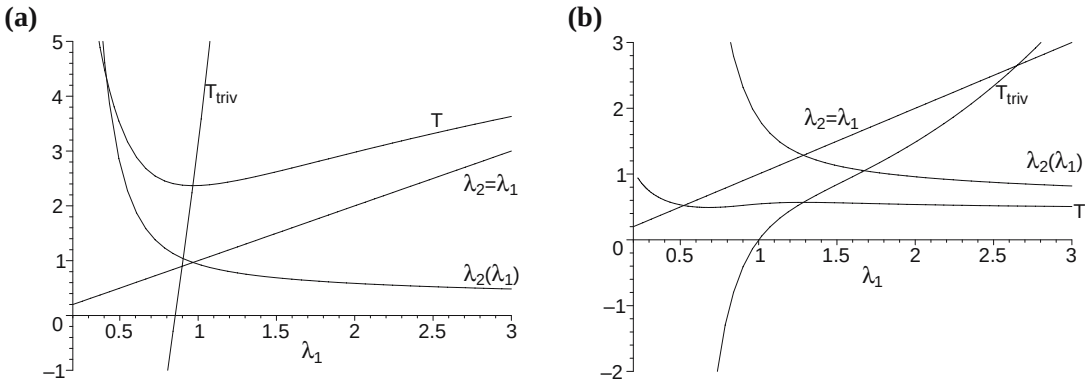

Figure 1. Plot of the deformation $\lambda_2(\lambda_1)$ and the loading T/μ for both the trivial and non-trivial solutions against λ_1. The material used is (32) with (a) $m=-4$, $\kappa/\mu=5$, $\lambda_3=1{\cdot}5$, (b) $m=-4$, $\kappa/\mu=5/4$, $\lambda_3=1$.

We now look at some numerical results for specific cases. In Figure 1a we plot two pairs of curves for the strain-energy function (32) with $m=-4$, $\lambda_3=1{\cdot}5$ and $\kappa/\mu=5$. This represents a very highly compressible material, something like foam rubber. Since there is a pre-stretch $\lambda_3=1{\cdot}5$ the trivial loading T will be zero for $\lambda_1=\lambda_2\simeq 0{\cdot}8539$. The straight line passing through the point $(3,3)$ is the trivial solution $\lambda_2=\lambda_1$ plotted against λ_1. The curve monotonically decreasing with λ_1 is the non-trivial deformation $\lambda_2(\lambda_1)$. These two curves intersect at the bifurcation point given by $\lambda_1=0{\cdot}9668$, approximately. The other pair of curves show the loading T/μ. The curve passing through the point $(0{\cdot}8539, 0)$ is the trivial loading with $\lambda_1=\lambda_2$ (T_{triv}). The remaining curve is the loading along the non-trivial path $T(\lambda_1, \lambda_2(\lambda_1))/\mu$. We note that these two curves intersect at a local minimum of the non-trivial loading, again at $\lambda_1\simeq 0{\cdot}9668$. This might be thought of as the usual or normal case where the plot of the two loading curves gives a pitchfork bifurcation. In Figure 1b we plot two pairs of curves for the strain-energy function (32) with $m=-4$, $\lambda_3=1$ and $\kappa/\mu=5/4$. The straight line passing through the point (2,2) is the trivial solution $\lambda_2=\lambda_1$ plotted against λ_1. The curve monotonically decreasing with λ_1 is the non-trivial deformation $\lambda_2(\lambda_1)$. These two curves intersect at the bifurcation point given by $\lambda_1\simeq 1{\cdot}285$. The other pair of curves show the loading T/μ. The curve passing through the point $\lambda_1=1$ is the trivial loading with $\lambda_1=\lambda_2$. We note that in this case these two curves intersect at a local maximum of the non-trivial loading, again at $\lambda_1\simeq 1{\cdot}285$. Here the non-trivial loading also exhibits two local minima. From (11) these occur at $\lambda_1\simeq 0{\cdot}684$ and $\lambda_1\simeq 5{\cdot}33$. In this case sub-critical non-trivial solutions exist which will inevitably lead to a more complicated stability picture. We shall investigate this below. Comparing Figure 1a and b we see that modest changes in the parameters can produce qualitatively different outcomes.

4. Exact stability analysis

Since we have dead loading or a rigid displacement on the boundary of the cube, the deformation will be stable if and only if the second variation of the energy is non negative. Starting with the total energy

$$E=\int_{\Omega} W\,\mathrm{d}V-\int_{S_1}\mathbf{T}.(\mathbf{x}-\mathbf{X})\,\mathrm{d}A, \tag{37}$$

where Ω is the volume of the cube in the reference configuration. The second integral is the work done by the traction $\mathbf{T}$ acting on the four sides S_1. Admissible variations $\dot{\mathbf{x}}$ are zero on the two sides perpendicular to the 3-direction. We then have

$$\dot{E} = \int_\Omega W_{\mathbf{F}}[\nabla\dot{\mathbf{x}}]\mathrm{d}V - \int_{S_1} \mathbf{T}.\dot{\mathbf{x}}\ \mathrm{d}A, \tag{38}$$

where a dot denotes the variation (increment) of a quantity and ∇ is the gradient operator in the reference configuration. Taking the second variation we have

$$\ddot{E} = \int_\Omega \{\nabla\dot{\mathbf{x}} \cdot W_{\mathbf{FF}}[\nabla\dot{\mathbf{x}}] + W_{\mathbf{F}}[\nabla\ddot{\mathbf{x}}]\}\ \mathrm{d}V - \int_{S_1} \mathbf{T}.\ddot{\mathbf{x}}\,\mathrm{d}A. \tag{39}$$

The second and third terms in (39) can be eliminated by a standard calculation. We do this by using the divergence theorem combined with the equilibrium equations, $\mathrm{Div}\, W_{\mathbf{F}} = \mathbf{0}$ and the boundary conditions $(W_{\mathbf{F}})^T\mathbf{N} = \mathbf{T}$ on S_1, where $\mathbf{N}$ is the unit outward normal. The stability condition then becomes

$$\ddot{E} = \int_\Omega \{\nabla\dot{\mathbf{x}} \cdot W_{\mathbf{FF}}[\nabla\dot{\mathbf{x}}]\}\ \mathrm{d}V > 0\,. \tag{40}$$

The quadratic integral inequality (40) will be used to determine the stability of the deformation $\mathbf{x}(\mathbf{X})$. The derivation of (40) is valid for deformations of general form. However, for the simple problem that we are considering the components of $W_{\mathbf{FF}}$ in (40) are all constants.

The second variation (40) is written in Lagrangian form and we continue with that formulation here. Let $u(X, Y)$ and $v(X, Y)$ be the first and second Cartesian components of the variation $\dot{\mathbf{x}}$. In the undeformed Cartesian coordinate system, $\nabla\dot{\mathbf{x}}$ has the following component form

$$\nabla\dot{\mathbf{x}} = \begin{pmatrix} u_X & u_Y & 0 \\ v_X & v_Y & 0 \\ 0 & 0 & 0 \end{pmatrix}, \tag{41}$$

where a subscript denotes the partial derivative. The non-zero components of $W_{\mathbf{FF}}$ are given by

$$(W_{\mathbf{FF}})_{iijj} = W_{ij}\,, \tag{42}$$

and

$$\left.\begin{aligned} (W_{\mathbf{FF}})_{ijij} = W_{ijij} &= \frac{\lambda_i W_i - \lambda_j W_j}{\lambda_i^2 - \lambda_j^2}\,, \\ (W_{\mathbf{FF}})_{ijji} = W_{ijji} &= \frac{\lambda_j W_i - \lambda_i W_j}{\lambda_i^2 - \lambda_j^2}\,, \end{aligned}\right\} \quad i \neq j\,, \quad \lambda_i \neq \lambda_j \tag{43}$$

with

$$\left.\begin{aligned} (W_{\mathbf{FF}})_{ijij} = W_{ijij} &= \left(\lambda_i W_{ii} - \lambda_i W_{ij} + W_i\right)/2\lambda_i\,, \\ (W_{\mathbf{FF}})_{ijji} = W_{ijji} &= \left(\lambda_i W_{ii} - \lambda_i W_{ij} - W_i\right)/2\lambda_i\,, \end{aligned}\right\} \quad i \neq j\,, \quad \lambda_i = \lambda_j\,, \tag{44}$$

where one or two subscripts on W denote partial differentiation with respect to λ_i. The case of four subscripts is just notation. We now find that the integrand in (40) can be written

$$\nabla\dot{\mathbf{x}} \cdot W_{\mathbf{FF}}[\nabla\dot{\mathbf{x}}] = W_{11}u_X^2 + W_{22}v_Y^2 + 2W_{12}u_X v_Y + W_{1212}(u_Y^2 + v_X^2) + 2W_{1221}u_Y v_X\,. \tag{45}$$

Since the coefficients of the incremental displacements in (45) are all constants, the deformation is stable if and only if

$$W_{11}\left(u_X+\frac{W_{12}}{W_{11}}v_Y\right)^2+v_Y^2\left(W_{22}-\frac{W_{12}^2}{W_{11}}\right)$$
$$+W_{1212}\left(u_Y+\frac{W_{1221}}{W_{1212}}v_X\right)^2+v_X^2\left(W_{1212}-\frac{W_{1221}^2}{W_{1212}}\right)>0\,,\quad W_{11}\neq 0\,. \tag{46}$$

We could, of course, write this in other ways. From (46) we deduce that the deformation is stable if and only if

$$W_{11}>0\,,\quad W_{22}>0\,,\quad W_{11}W_{22}-W_{12}^2>0\,,\quad W_{1212}^2-W_{1221}^2>0\,, \tag{47}$$

since $W_{1212}>0$ by the Baker–Ericksen inequalities [15, p. 343].

In the preceeding sections, we have derived a general bifurcation equation (29) and the stability condition that (45) be positive definite. In order to make a direct comparison we rewrite the stability condition (40) using Eulerian variables. We have

$$\nabla\dot{\mathbf{x}}=\boldsymbol{\eta}\mathbf{F}\,, \tag{48}$$

and in Cartesian component form we can write

$$(W_{\mathbf{FF}})_{ijkl}=J\,F_{jp}^{-1}F_{lq}^{-1}B_{piqk}\,, \tag{49}$$

which follows from (16) and (42–44), see also Ogden [5, Equation 6.1.29]. Hence we can write

$$\ddot{E}=\int_\Omega\{\nabla\dot{\mathbf{x}}\cdot W_{\mathbf{FF}}[\nabla\dot{\mathbf{x}}]\}\mathrm{d}V=\int_{\Omega_0}\{\eta_{ji}B_{ijkl}\eta_{lk}\}\mathrm{d}v, \tag{50}$$

where Ω_0 is the volume of the body in the current configuration.

We note that at a bifurcation point incremental equilibrium equations (13) with (15) are satisfied. Hence

$$\dot{\mathbf{x}}\cdot\mathrm{div}\,\dot{\mathbf{s}}_o=\dot{x}_j\frac{\partial}{\partial x_i}(B_{ijkl}\eta_{lk})=0\,. \tag{51}$$

If we integrate over the current volume

$$0=\int_{\Omega_0}\dot{x}_j\frac{\partial}{\partial x_i}\left(B_{ijkl}\eta_{lk}\right)\,\mathrm{d}v=\int_{\Omega_0}\frac{\partial}{\partial x_i}\left(\dot{x}_jB_{ijkl}\eta_{lk}\right)\,\mathrm{d}v-\int_{\Omega_0}\eta_{ji}B_{ijkl}\eta_{lk}\,\mathrm{d}v\,. \tag{52}$$

Now using the divergence theorem and (15) we find that

$$0=\int_{\partial\Omega_0}\left(\dot{x}_jB_{ijkl}\eta_{lk}\right)n_i\,\mathrm{d}a-\int_{\Omega_0}\eta_{ji}B_{ijkl}\eta_{lk}\,\mathrm{d}v$$
$$=\int_{\partial\Omega_0}\dot{x}_j\,\dot{s}_{oij}n_i\,\mathrm{d}a-\int_{\Omega_0}\eta_{ji}B_{ijkl}\eta_{lk}\,\mathrm{d}v\,. \tag{53}$$

The variation $\dot{\mathbf{x}}$ satisfies the same boundary conditions as the incremental displacement used in the bifurcation problem, (20) and (21). The first term in $(53)_2$ is identically zero and so (50) is zero at a bifurcation point. Hence every bifurcation point is neutrally stable.

4.1. Stability of the trivial solution

Firstly, we consider the stability of the trivial solution $\lambda_1 = \lambda_2 = \lambda$. In this case we use $W_{11} \equiv W_{22}$ and (44) to write (47) as

$$W_1 > 0\,, \quad W_{11} > 0\,, \quad W_{11} \pm W_{12} > 0\,. \tag{54}$$

We note that the cube appears to be unstable under compression. However, the post bifurcation solution in this case corresponds to a incremental rotation; see [16, 17] for a discussion of this instability. We are concerned with a tensile loading and so we require

$$W_{11} > 0\,, \quad W_{11} \pm W_{12} > 0\,. \tag{55}$$

The three modes for failure of stability are readily identified. If $W_{11} = 0$ we have a loss of ellipticity, the square external shape is maintained but the deformation becomes inhomogeneous. This may be excluded by constitutive assumptions made about reasonable material behaviour. Secondly, if $W_{11} + W_{12} = 0$ we have from (12) a local turning point of the (trivial) loading T. The first such turning point to be encountered will of course be a local maximum. While this is technically an instability there is no associated bifurcation and such an event would usually bring into question the appropriateness of the material model. Finally, if $W_{11} - W_{12} = 0$ we have the bifurcation point (7) where the square cross section becomes unstable and there is a rectangular alternative. This will also correspond to a turning point of the non-trivial loading (11). It is possible to construct examples where $W_{11} = 0$ before, at or after the bifurcation point. We may also have $W_{11} = 0$ when there is no bifurcation point. Hence the trivial solution may become unstable without a bifurcation point or before or after a bifurcation point. Similarly, there is no connection between turning points of the trivial loading and bifurcation points. We look at the materials used to plot Figure 1a and b.

4.1.1. *Case 1*

Here we have (32) with (33) and

$$m = -4\,, \quad \kappa/\mu = 5\,, \quad \lambda_3 = 1.5\,. \tag{56}$$

It then follows that

$$\begin{aligned} W_{11} &= \mu\left(20\lambda^{-6} + 69\lambda^2\right)/8 > 0\,, \\ W_{11} + W_{12} &= \mu\left(20\lambda^{-6} + 207\lambda^2 - 40\right)/8\,, \\ W_{11} - W_{12} &= \mu\left(20\lambda^{-6} - 69\lambda^2 + 40\right)/8\,. \end{aligned} \tag{57}$$

Since $\lambda_3 = 1{\cdot}5$ we have $\lambda \simeq 0{\cdot}854$ when there is no lateral loading. As the loading is increased we see from (57_2) that $W_{11} + W_{12} > 0$ and that there is a single bifurcation point ($W_{11} - W_{12} = 0$ at $\lambda \simeq 0{\cdot}9668$) where the square cross-sectional shape becomes unstable.

4.1.2. *Case 2*

We again have (32) with (33) but

$$m = -4\,, \quad \kappa/\mu = 5/4\,, \quad \lambda_3 = 1\,. \tag{58}$$

We now have

$$W_{11}=\mu\frac{(30+\lambda^8)}{12\lambda^6}>0\,,\quad W_{11}+W_{12}=\mu\frac{(30+3\lambda^8+5\lambda^6)}{12\lambda^6}>0\,,$$
$$W_{11}-W_{12}=\mu\frac{(30-\lambda^8-5\lambda^6)}{12\lambda^6}\,. \tag{59}$$

Clearly, there is again a single bifurcation point ($W_{11}=W_{12}$ at $\lambda\simeq 1{\cdot}285$) where the square cross-sectional shape becomes unstable and the cube assumes a general parallelogram shape.

To demonstrate some slightly more complicated behaviour on the trivial solution we consider a third set of parameters.

4.1.3. *Case 3*

We start again with (32) and (33) but take

$$m=-4\,,\quad \kappa/\mu=1\,,\quad \lambda_3=1\,. \tag{60}$$

In this case

$$W_{11}=\mu\frac{(15-\lambda^8)}{6\lambda^6}\,,\quad W_{11}+W_{12}=\mu\frac{(15-3\lambda^8+4\lambda^6)}{6\lambda^6}\,,\quad W_{11}-W_{12}=\mu\frac{(15+\lambda^8-4\lambda^6)}{6\lambda^6} \tag{61}$$

For this combination of parameters we find two bifurcation points at $\lambda\simeq 1{\cdot}392$, and $\lambda\simeq 1{\cdot}925$. Interestingly, we also have $W_{11}+W_{12}=0$ at $\lambda\simeq 1{\cdot}407$, and $W_{11}=0$ at $\lambda=15^{1/8}\simeq 1{\cdot}403$. To illustrate, we plot in Figure 2 the same quantities as those shown in Figure 1a and b. In particular the upper portion of Figure 2 comprises the trivial deformation, which is the straight line $\lambda_1=\lambda_2=\lambda$, and the closed curve of the non-trivial deformation $\lambda_2(\lambda_1)$. We see that there is only a finite interval for λ_1 for which solutions $\lambda_2\neq\lambda_1$ exist. The intersection of the trivial and non-trivial solutions give the two bifurcation points. In the lower part of Figure 2 we plot the corresponding loading (scaled by a factor of $2\mu/5$). The closed curve is the non-trivial solution while the parabolic shaped curve which becomes negative is the trivial loading solution. In this case we see that one bifurcation point occurs at a local maximum of the non-trivial loading and the other at a local minimum. The trivial loading path also has a

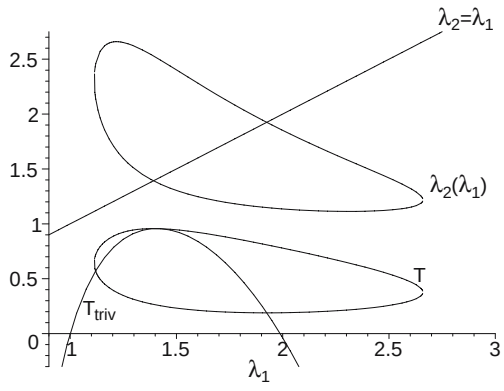

Figure 2. Plot of the deformation $\lambda_2(\lambda_1)$ and the loading $5T/2\mu$ for both the trivial and non-trivial solutions against λ_1. The material used is (32) with $m=-4$, $\kappa=\mu$ and $\lambda_3=1$.

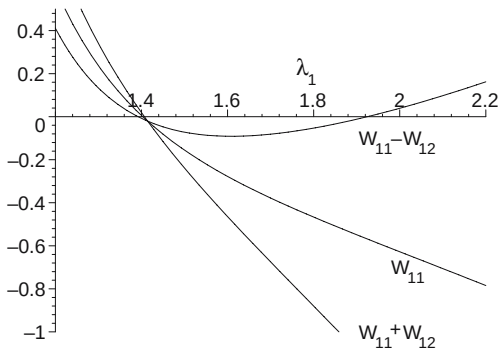

Figure 3. Plot W_{11}, $W_{11}+W_{12}$ and $W_{11}-W_{12}$ of against λ_1 along the trivial solution. The material used is (32) with $m=-4$, $\kappa=\mu$ and $\lambda_3=1$.

local maximum (not distinguished from that of the non-trivial local maximum with the scale used in Figure 2) but is in fact slightly higher and later than that of the non-trivial one. We also note that the two loading paths have a third point of intersection ($\lambda_1 \simeq 1{\cdot}1196$). This does not, however, indicate a third bifurcation point. As can be seen from the deformation paths in the upper part of Figure 2 the trivial and non-trivial deformations at this point are quite different. This third point of intersection of the loading paths offers the possibility of a snap-through instability. Finally, we note that for this combination of parameters there is a maximum load that can be sustained, $W_{11}+W_{12}=0$ at $\lambda \simeq 1{\cdot}407$, which, along with the loss of strong ellipticity ($W_{11}=0$ at $\lambda = 15^{1/8}$), may just indicate that it is not a physically meaningful example.

To get a clear picture of the stability of the different parts of the trivial loading we plot in Figure 3 the curves of W_{11}, $W_{11} \pm W_{12}$ which have henceforth been non-dimensionalised by taking $\mu = 1$. We see that $W_{11} - W_{12}$ has two roots corresponding to the two bifurcation points. However, at least one of the curves plotted is negative after the first bifurcation point and so the trivial solution is unstable after this point, the second bifurcation point does not return us to a stable (trivial) configuration.

4.2. Stability of the non-trivial solution

To obtain the non-trivial solution we first solve (6) for $\lambda_2 = \lambda_2(\lambda_1)$ and then use this for any further calculations. For $\lambda_1 \neq \lambda_2$ the stability criteria (47) fails since, from (43) with $W_1 = W_2$ we have $W_{1221} = -W_{1212}$. Hence all non-trivial solutions are neutrally stable at best. This was also found to be the case for incompressible materials; see [5, Section 6.3.2]. For neutral stability (rather than instability) we then require

$$W_{11} \geq 0\,, \quad W_{22} \geq 0\,, \quad W_{11}W_{22} - W_{12}^2 \geq 0\,. \tag{62}$$

4.2.1. *Case 1*

Here the material parameters are given by (56). This is the most straightforward case of a simple pitchfork type bifurcation. We recall from Figure 1a that the non-trivial loading has a single simple local minimum at the single bifurcation point. In Figure 4 we plot the non-dimensionalised curves of W_{11}, W_{22} and $W_{11}W_{22} - W_{12}^2$. We see from Figure 4 that the entire non-trivial loading is neutrally stable it does not become unstable. For this particular case we then have a standard result. The trivial solution is followed until the bifurcation point and then one of the non-trivial branches becomes the preferred solution.

4.2.2. *Case 2*

In this case the material parameters are given by (58). In Figure 5 we plot the curves of W_{11}, W_{22} and $W_{11}W_{22} - W_{12}^2$. We see that W_{11} and W_{22} are always positive and so ellipticity is maintained and this does not effect the stability of the body. However $W_{11}W_{22} - W_{12}^2$ has a local maximum (of zero) at the bifurcation point. It also has two other zero's at the two turning points of the non-trivial loading T; see Figure 1b. Hence we can deduce that the non-trivial loading is unstable in the neighbourhood of the bifurcation point and remains unstable until the loading reaches a local minimum at which point the non-trivial deformation becomes neutrally stable. Here we would expect the loading to follow the stable trivial solution as far as the bifurcation point. The solution will then jump (horizontally in Figure 1b) to one of the neutrally stable non-trivial branches with the same numerical value of the load.

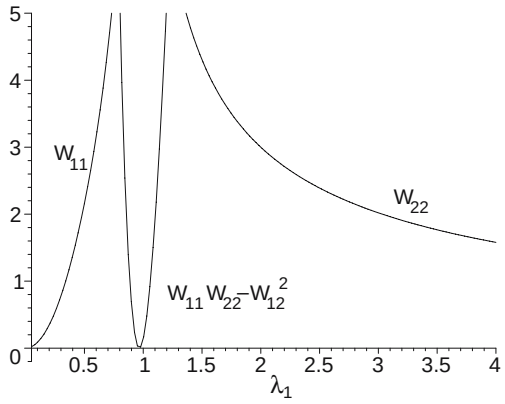

Figure 4. Plot W_{11}, W_{22} and $W_{11}W_{22} - W_{12}^2$ of against λ_1 along the non-trivial solution path. The material used is (32) with (33) and (56).

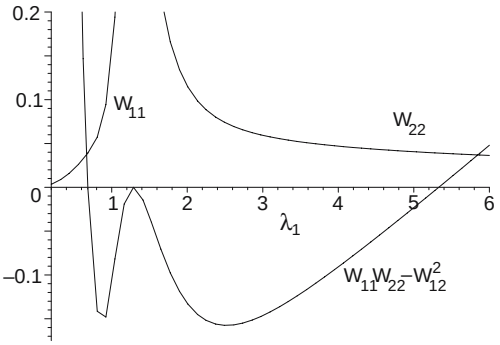

Figure 5. Plot W_{11}, W_{22} and $W_{11}W_{22} - W_{12}^2$ of against λ_1 along the non-trivial solution path. The material used is (32) with (33) and (58).

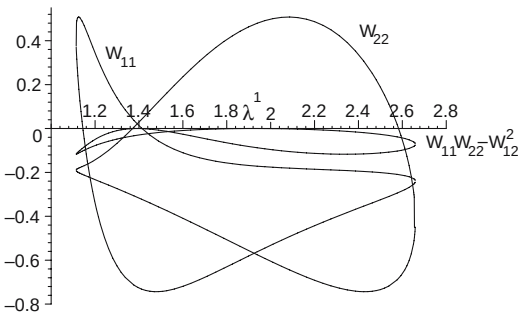

Figure 6. Plot W_{11}, W_{22} and $W_{11}W_{22} - W_{12}^2$ of against λ_1 along the non-trivial solution path. The material used is (32) with (33) and (60).

4.2.3. *Case 3*

Here the strain-energy function is again (32) and (33) with parameters (60). In this case $\lambda_2(\lambda_1)$ formes a closed curve, as shown in Figure 2 above. In Figure 6 we plot the three curves of W_{11}, W_{22} and $W_{11}W_{22} - W_{12}^2$ which are also closed curves. Obviously one or more of these curves are negative throughout the range of existence of the non-trivial solution and so it is always unstable. We see that the flat sideways figure of eight curve for $W_{11}W_{22} - W_{12}^2$ has two double zero's at the bifurcation points. For case three a comparison of Figures 2, 3 and 6 give the overall deformation and stability results. As we increase the loading from the undeformed configuration the trivial solution is stable. At the first bifurcation point ($\lambda \simeq 1{\cdot}392$) this becomes unstable but the rectangular non-trivial solution is also unstable. Perhaps this is not surprising given that there is a global maximum attainable load.

5. Alternative stability analysis

We now apply the method introduced by Chen and Haughton [12]. This is of course not necessary for this problem. However, it affords the opportunity to look at the resulting differential equations when the stability results are known from that presented above.

The inequality (40) with (45) involves the integral of a quadratic function of two perturbations u and v. We shall impose the boundary conditions used for the bifurcation analysis (20). First we expand the functions $u(X,Y)$ and $v(X,Y)$ into series in Y:

$$u(X,Y)=\frac{f_0(X)}{2}+\sum_{n=1}^{\infty} f_n(X)\cos\bar{\alpha}Y, \tag{63}$$

$$v(X,Y)=\sum_{n=1}^{\infty} g_n(X)\sin\frac{n\pi Y}{A}=\sum_{n=1}^{\infty} g_n(X)\sin\bar{\alpha}Y. \tag{64}$$

After a little work the stability criterion (40) with (45) can then be written as

$$\int_0^A\Big[\sum_{n=1}^{\infty}\{W_{11}(f')^2-2\bar{\alpha}(W_{1221}fg'-W_{12}f'g)+\bar{\alpha}^2(W_{22}g^2+W_{1212}f^2)+W_{1212}(g')^2\}$$
$$+\frac{W_{11}(f_0')^2}{2A}\Big]\mathrm{d}X>0, \tag{65}$$

where we have now omitted the subscript n from f and g and a dash indicates differentiation with respect to X.

We shall consider the different mode numbers n individually. Firstly, for $n=0$ the stability criterion (65) reduces to

$$W_{11}\int_0^A (f_0')^2\,\mathrm{d}X>0, \tag{66}$$

and hence we recover (47_1) the strong ellipticity condition. For the general case $n>0$ we now introduce arbitrary functions (integrating factors) $y_i(X)$, $i=1,2,3$, and write (65) as

$$\int_0^A\sum_{n=1}^{\infty}\Big\{\Gamma_1^2+\Gamma_2^2+2y_1f'f+2y_2(f'g+fg')+2y_3g'g$$
$$+f^2\left(\bar{\alpha}^2W_{1212}-\frac{y_1^2}{W_{11}}-\frac{(\bar{\alpha}W_{1221}+y_2)^2}{W_{1212}}\right)$$
$$+2fg\left(\frac{y_1(\bar{\alpha}W_{12}-y_2)}{W_{11}}-\frac{y_3(\bar{\alpha}W_{1221}+y_2)}{W_{1212}}\right)$$
$$+g^2\left(\bar{\alpha}^2W_{22}-\frac{(\bar{\alpha}W_{12}-y_2)^2}{W_{11}}-\frac{y_3^2}{W_{1212}}\right)\Big\}\mathrm{d}X>0, \tag{67}$$

where

$$\Gamma_1=\frac{1}{\sqrt{W_{11}}}\left(W_{11}f'-y_1f+(\bar{\alpha}W_{12}-y_2)g\right),\quad W_{11}>0,$$
$$\Gamma_2=\frac{1}{\sqrt{W_{1212}}}\left(W_{12121}g'-y_3g-(\bar{\alpha}W_{1221}+y_2)f\right). \tag{68}$$

Recall that the Baker-Ericksen inequalities give $W_{1212}>0$. Since the y_i's are arbitrary, we may now set

$$y_1'=\bar{\alpha}^2W_{1212}-\frac{y_1^2}{W_{11}}-\frac{(\bar{\alpha}W_{1221}+y_2)^2}{W_{1212}},$$
$$y_2'=\frac{y_1(\bar{\alpha}W_{12}-y_2)}{W_{11}}-\frac{y_3(\bar{\alpha}W_{1221}+y_2)}{W_{1212}}, \tag{69}$$
$$y_3'=\bar{\alpha}^2W_{22}-\frac{(\bar{\alpha}W_{12}-y_2)^2}{W_{11}}-\frac{y_3^2}{W_{1212}}$$

with

$$y_i(0)=0, \quad i=1,2,3. \tag{70}$$

Substituting (69) in (67) we have the stability criterion

$$\int_0^A \{\Gamma_1^2+\Gamma_2^2+f^2y_1'+g^2y_3'+2fgy_2'+2y_1f'f+2y_2(f'g+fg')+2y_3g'g\}\,\mathrm{d}X>0\,, \tag{71}$$

where we now have implied summation over n. Integrating by parts and using (70) we finally have the stability criterion in the form

$$\int_0^A \{\Gamma_1^2+\Gamma_2^2\}\,\mathrm{d}X+\left[f^2y_1+2fgy_2+g^2y_3\right]\Big|_A>0\,. \tag{72}$$

For stability of the deformed body it is clearly sufficient for the matrix

$$\begin{pmatrix} y_1(A) & y_2(A) \\ y_2(A) & y_3(A) \end{pmatrix} \tag{73}$$

to be positive semi-definite. It is also easy to see that this condition is necessary. If (73) is not positive semi-definite then there are numbers p and q such that

$$p^2y_1(A)+q^2y_3(A)+2pqy_2(A)<0.$$

We can then choose f, g to be functions which make Γ_1 and Γ_2 identically zero, see (58), with $f(A)=p$, $g(A)=q$. In this case $\ddot{E}<0$.

The problem of assessing the full non-linear stability of a body in a particular configuration then reduces to that of solving the initial-value problem (69) with (70) and evaluating the matrix (73). This is in principle a straightforward calculation. We can determine any change in stability to within the accuracy of the numerical methods used.

6. Comparison of stability results

In this section, we present some calculations to compare the stability condition, the positive definiteness of (73), with known results.

Firstly, we make a change of variables;

$$s=\bar{\alpha}\,X\,, \quad y_i(X)=\bar{\alpha}\,Y_i(s)\,, \tag{74}$$

so that (69) and (70) become

$$\begin{aligned} Y_1' &= W_{1212}-\frac{Y_1^2}{W_{11}}-\frac{(W_{1221}+Y_2)^2}{W_{1212}}, \\ Y_2' &= \frac{Y_1(W_{12}-Y_2)}{W_{11}}-\frac{Y_3(W_{1221}+Y_2)}{W_{1212}}, \\ Y_3' &= W_{22}-\frac{(W_{12}-Y_2)^2}{W_{11}}-\frac{Y_3^2}{W_{1212}}, \end{aligned} \tag{75}$$

where a prime now denotes differentiation with respect to s. The initial conditions are

$$Y_i(0)=0, \quad i=1,2,3. \tag{76}$$

The stability criterion, positive definite matrix (73), can then be written

$$Y_1(n\pi) > 0\,, \quad Y_3(n\pi) > 0\,, \quad Y_1(n\pi)Y_3(n\pi) - Y_2^2(n\pi) > 0\,. \tag{77}$$

It is now clear that the physical dimensions (A) of the block play no part in the stability of the deformation, as we would expect. We now focus attention on the case $n=1$.

If we rewrite (75) in the form

$$\begin{aligned} Y_1' &= \frac{(W_{1212}^2 - W_{1221}^2)}{W_{1212}} - \frac{Y_1^2}{W_{11}} - \frac{Y_2(2W_{1221} + Y_2)}{W_{1212}}, \\ Y_2' &= \frac{Y_1(W_{12} - Y_2)}{W_{11}} - \frac{Y_3(W_{1221} + Y_2)}{W_{1212}}, \\ Y_3' &= \frac{(W_{11}W_{22} - W_{12}^2)}{W_{11}} + \frac{(2W_{12} - Y_2)Y_2}{W_{11}} - \frac{Y_3^2}{W_{1212}}, \end{aligned} \tag{78}$$

then it is easy to see that there is a solution $Y_i \equiv 0$ at

$$\frac{(W_{1212}^2 - W_{1221}^2)}{W_{1212}} = 0 \quad \text{and} \quad \frac{(W_{11}W_{22} - W_{12}^2)}{W_{11}} = 0\,. \tag{79}$$

In general we will have only one parameter at our disposal at this stage (λ_1) and so it will only be in exceptional cases that we will be able to satisfy both conditions in (79) simultaneously. However, on the trivial solution we have $W_{11} \equiv W_{22}$ and, from (44), $W_{1212}^2 - W_{1221}^2 = W_1(W_{11} - W_{12})/\lambda$. Hence we can see that, on the trivial solution, (79) is $W_{11} = \pm W_{12}$. We then have either a bifurcation point, (7), or a turning point of the trivial loading (12). This is then the mechanism whereby any bifurcation point is neutrally stable. For other (inhomogeneous) problems that we have considered using this method [12–14], this particular type of solution was not available.

6.1. Numerical results

6.1.1. *Case 1*

The numerical solution of (75) with (76) to evaluate $Y_i(\pi)$ is surprisingly difficult. Starting with the initial configuration $\lambda_3 = 1{\cdot}5$ and zero lateral loading ($\lambda_1 = \lambda_2 \simeq 0{\cdot}854$) we find that $Y_1(\pi) \simeq Y_3(\pi) \simeq 3{\cdot}2$, $Y_2(\pi) \simeq -0{\cdot}25$ and $Y_1(\pi)Y_3(\pi) - Y_2^2(\pi) \simeq 10{\cdot}5$, having non-dimensionalised Y_i with respect to μ. All three curves are then monotonically decreasing towards zero at the bifurcation point. In Figure 7a we plot the curves of $Y_1(\pi)$ and the determinant $Y_1(\pi)Y_3(\pi) - Y_2^2(\pi)$ near the bifurcation point. ($Y_3(\pi)$ is virtually indistinguishable from $Y_1(\pi)$ and so it has been omitted for clarity). As can be seen from Figure 7a $Y_1(\pi)$ and $Y_3(\pi)$ both have simple zero's at the bifurcation point while the determinant has a double root. Also from Figure 7a we see that $Y_1(\pi)$ and $Y_3(\pi)$ quickly become very large and negative as λ_1 is increased. We also find that $Y_2(\pi)$ becomes very large and negative. The numerical methods that we have tried all fail to find $Y_i(\pi)$ with any reasonable accuracy once λ_1 is increased much beyond the bifurcation point. However, it is easy to see from (75) that once we have $Y_1(\pi)$ and $Y_3(\pi)$ large (and negative) compared to the constant terms in (75) and $Y_2(\pi)$ is large and negative then this situation will persist for finite changes in λ_1. This then allows us to deduce that the trivial solution will be unstable for all values of λ_1 greater than the bifurcation value.

If we now consider the non-trivial solution path we find that the numerical calculations are much simpler. In Figure 7b we plot the stability curves. As can be seen there is no singular behaviour. As λ_1 becomes large $Y_1(\pi)$ and $Y_2(\pi)$ appear to approach asymptotes while $Y_3(\pi)$ increases no more than linearly with λ_1. As can be seen, all curves are positive apart from zero's at the bifurcation point and so the non-trivial solution is neutrally stable.

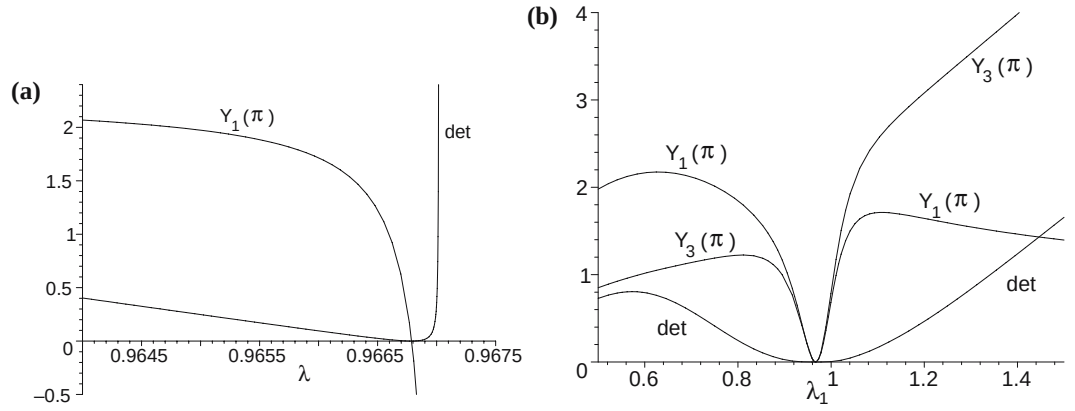

Figure 7. Plot of $Y_1(\pi)$, $Y_3(\pi)$ and $Y_1(\pi)Y_3(\pi) - Y_2^2(\pi)$ for material (32) with $m = -4$, $\kappa/\mu = 5$ and $\lambda_3 = 1{\cdot}5$: (a) on the trivial path, (b) on the non-trivial path.

6.1.2. *Case 2*

From Figures 1b and 5 there are three points of interest which correspond to the three turning points of the non-trivial loading. Firstly, on the trivial solution we increase λ_1 from its initial value of unity and calculate the resulting values of $Y_1(\pi) \simeq Y_3(\pi)$ and $Y_1(\pi)Y_3(\pi) - Y_2^2(\pi)$. Initially $Y_i(\pi)$, i=1,2,3 all take values between zero and 1·5. The determinant is positive and so we have a stable configuration. As λ_1 is increased $Y_1(\pi)$ and $Y_3(\pi)$ have simple zero's and the determinant has a double root at the bifurcation point. After this point $Y_1(\pi)$ and $Y_3(\pi)$ quickly become large and negative while the determinant becomes large and positive. We have a similar plot to that of Figure 7a.

We now look at the non-trivial solution path. In Figure 8a we plot values of $Y_1(\pi)$, $Y_3(\pi)$ and $75(Y_1(\pi)Y_3(\pi) - Y_2^2(\pi))$ in the neighbourhood of the first turning point of the non-trivial loading curve ($\lambda_1 \simeq 0{\cdot}684$), see Figure 1b. We note that $Y_1(\pi)$ and $Y_3(\pi)$ have simple zeros while the determinant (multiplied by 75 for clarity) has a double root. The non-trivial loading between the first local minimum and maximum (bifurcation point) is then unstable. The loading to the left of the first minimum is neutrally stable. $Y_i(\pi)$ become large and incalculable as λ_1 increases. However, as we approach the bifurcation point ($\lambda_1 \simeq 1{\cdot}285$) we have details as shown in Figure 8b. Both $Y_1(\pi)$ and $Y_3(\pi)$ have local maxima of zero while the determinant has a local minimum of zero. The negative values of $Y_1(\pi)$ and $Y_3(\pi)$ means that the

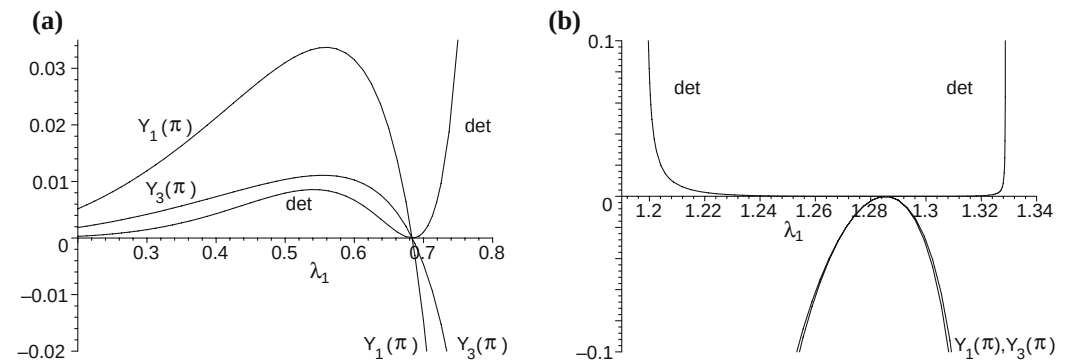

Figure 8. Plot of $Y_1(\pi)$, $Y_3(\pi)$ and $75(Y_1(\pi)Y_3(\pi) - Y_2^2(\pi))$ on the non-trivial solution from (75) with (76) for material (32) with $m = -4$, $\kappa/\mu = 5/4$, $\lambda_3 = 1$: (a) near local maximum, (b) near the bifurcation point.

solution continues to be unstable. Finally as we approach the second turning point of the non-trivial loading $\lambda_1 \simeq 5{\cdot}33$ we again find the numerical method breaks down. By choosing a small enough interval around the turning point we can confirm that $Y_1(\pi)$, $Y_3(\pi)$ and $Y_1(\pi)Y_3(\pi) - Y_2^2(\pi)$ are all positive after the turning point, as the exact stability analysis indicated, see Figure 5 and the discussion of it.

6.1.3. *Case 3*

In Figure 9 we plot the stability curves around the first bifurcation point ($\lambda_1 = 1{\cdot}392$) on the trivial solution path. We note that we have a loss of ellipticity ($W_{11} = 0$) at $\lambda_1 = 1{\cdot}403$ which reverses the signs of $Y_i(\pi)$ as they pass through a vertical asymptote. There is also a trivial loading maximum $W_{11} + W_{12} = 0$ at $\lambda_1 = 1{\cdot}407$. In Figure 9 the almost vertical lines of $Y_1(\pi) \simeq Y_3(\pi)$ are both moving from positive to negative values as λ_1 increases. Clearly, the differential equations pick out the loss of stability at the first bifurcation point $\lambda_1 \simeq 1{\cdot}392$. Using a finer scale we find that we have a picture qualitatively similar to that shown in Figure 7a. It is also easy to conclude that the solution is unstable after $\lambda_1 \simeq 1{\cdot}404$. However, using a finer scale we find that there are three distinct zeros around this point, successively, one for each of $Y_1(\pi)$, $Y_3(\pi)$ and the determinant.

If we increase λ_1 on the trivial solution path towards the second bifurcation point ($\lambda_1 \simeq 1{\cdot}925$ we obtain the stability curves shown in Figure 10. The determinant has a double root and both Y_1 and Y_3 have simple roots at the bifurcation point. However, we see that there is a region where all three curves are positive which would indicate a stable solution if we did not have $W_{11} < 0$. This seems to suggest the loss of ellipticity makes the method unreliable. Of course the method is originally set up with the assumption that $W_{11} > 0$, see (68), and it seems that we cannot just push the numerical calculations past this value. We can only determine stability in an elliptic regime which is not really a drawback since deformations where ellipticity is lost will be unstable by definition.

If we move on to the non-trivial solution then we can plot two versions of the stability curves depending on which of the two solutions for $\lambda_2(\lambda_1)$ that we choose; see Figure 2. At the first bifurcation point we have the results shown in Figure 11. The horizontal non-zero curve is $Y_1(\pi)Y_3(\pi) - Y_2^2(\pi)$ evaluated for the upper λ_2 solution. Both $Y_1(\pi)$, and $Y_3(\pi)$ for the upper solution are positive but out of the range of Figure 11. The U-shaped curve is the determinant for the lower solution and the negative curve corresponds to both $Y_1(\pi)$ and $Y_3(\pi)$ for the lower solution. Since $Y_1(\pi)$ and $Y_3(\pi)$ are negative on either side of the bifurcation point this branch of the non-trivial solution is unstable. But the fact that $Y_1(\pi)$, $Y_3(\pi)$

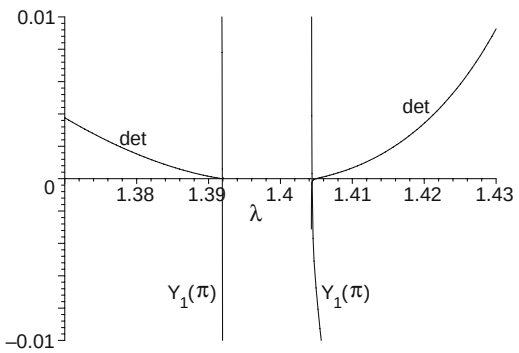

Figure 9. Plot of $Y_1(\pi) \simeq Y_3(\pi)$ and $Y_1(\pi)Y_3(\pi) - Y_2^2(\pi)$ on the trivial solution from (75) with (76) for material (32) with (60).

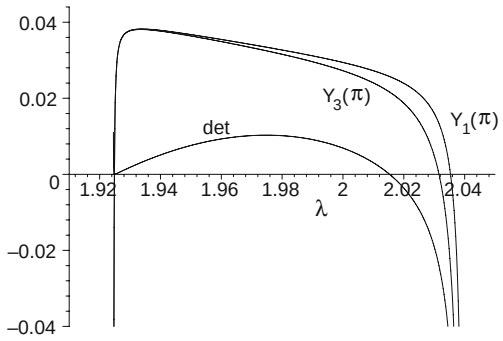

Figure 10. Plot of $Y_1(\pi)$, $Y_3(\pi)$ and $10(Y_1(\pi)Y_3(\pi) - Y_2^2(\pi))$ on the trivial solution from (75) with (76) for material (32) with (60) near the second bifurcation point $\lambda_1 \simeq 1{\cdot}925$.

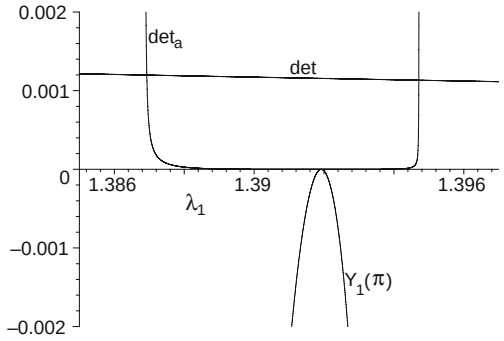

Figure 11. Plot of $Y_1(\pi) \simeq Y_3(\pi)$ and $Y_1(\pi)Y_3(\pi) - Y_2^2(\pi)$ on the non-trivial solution from (75) with (76) for material (32) with (60). The non-trivial solution is double-valued.

and the determinant are positive on the upper branch suggests that this solution is stable. This contradicts the exact stability results shown in Figure 5 where $W_{11}W_{22} - W_{12}^2 < 0$ for all nontrivial solutions and so they are unstable. The explanation for this is again the sign of W_{11}. In Figure 5 the lower portion of the W_{11} curve corresponds to the upper branch of the $\lambda_2(\lambda_1)$ curve. Hence for the range of Figure 11 $W_{11} < 0$ for the upper branch and the stability equations are not valid.

Finally, if we approach the second bifurcation point we find that all of the stability curves $Y_i(\pi)$ and the determinants are positive. This again contradicts the exact stability results but we now have $W_{11} < 0$ for both branches of the non-trivial solution as can be seen in Figure 5.

7. Conclusions

We have seen that the bifurcation and stability analysis for the two dimensional plain strain version of Rivlin's cube for compressible materials is straightforward. For an arbitrary material quite general results can be found. We have shown that bifurcation points are neutrally stable and must occur at turning points of the non-trivial loading. We have also found that the non-trivial deformation is at best neutrally stable. This is also the case for incompressible materials, [5]. Finally we have shown that the non-trivial (post-bifurcation) path can change from being neutrally stable to being unstable only at turning points of the loading. By choosing the class of strain-energy functions (32) a wide range of behaviour can be found in a relatively small range of constitutive parameters.

For the stability method of Chen and Haughton [12] we have found several interesting results. Firstly, the setting up of the problem requires attention. In particular it is not possible to obtain reliable results if ellipticity has been lost and this is evident from the form of the original argument of the second variation. Numerical calculations are routine for moderate deformations in the elliptic regime up to bifurcation points but can become difficult for larger deformations. It may be possible to extend the range of useful results by a re-scaling of the equations but we have not attempted that here. Our calculations here and in previous work suggest that it is the determinant (of the stability matrix) that will determine the stability of the deformation. The zeros of leading minors will play a role only in special cases. Since the determinant assumes the dominant role the numerical methods used should anticipate this.

The method given in [12–14] is quite general and its use is not restricted to nonlinear elasticity. Any analysis of a second variation can, at least potentially, benefit from an appropriate application of the method. We plan to look at other problems from a variety of different sources in the future.

Acknowledgement

The author would like to thank the referees for helpful suggestions and for bringing [11] to his attention.

References

1. R.S. Rivlin, Large elastic deformations of isotropic materials. II. Some uniqueness theorems for pure homogeneous deformation. *Phil. Trans. R. Soc. London* A 240 (1948) 491–508.
2. R.S. Rivlin, Stability of pure homogeneous deformations of an elastic cube under dead loading. *Q. Appl. Math.* 32 (1974) 265–271.
3. C.H. Wu and O.E. Widera, Stability of a thick rubber solid subject to pressure loads. *Int. J. Solids Struct.* 5 (1969) 1107–1117.
4. K.N. Sawyers and R.S. Rivlin, Bifurcation conditions for a thick elastic plate under thrust. *Int. J. Solids Struct.* 10 (1974) 483–501.
5. R.W. Ogden, *Non-Linear Elastic Deformations*. New York: Dover Publications. (1997) 532 pp.
6. R.W. Ogden, Local and global bifurcation phenomena in plane strain finite elasticity. *Int. J. Solids Struct.* 21 (1985) 121–132.
7. C.E. Pearson, General theory of elastic stability. *Q. Appl. Math.* 14 (1956) 133–144.
8. R. Hill, On uniqueness and stability in the theory of finite elastic strain. *J. Mech. Phys. Solids* 5 (1957) 229–241.
9. K.N. Sawyers and R.S. Rivlin, Stability of a thick elastic plate under thrust. *J. Elasticity* 12 (1982) 101–125.
10. R.W. Ogden, On non-uniqueness in the traction boundary-value problem for a compressible elastic solid. *Q. Appl. Math.* 42 (1984) 337–344.
11. R.S. Rivlin and M.F. Beatty, Dead loading of a unit cube of compressible isotropic elastic material. *Z.A.M.P.* 54 (2003) 954–963.
12. Y.C. Chen and D.M. Haughton, Stability and bifurcation of inflation of elastic cylinders. *Proc. R. Soc. London* A459 (2003) 137–156.
13. D.M. Haughton, On non-linear stability in unconstrained non-linear elasticity. *Int. J. Non-Linear Mech.* 39 (2004) 1181–1192.
14. D.M. Haughton and E. Kirkinis, A comparison of stability and bifurcation criteria for inflated spherical elastic shells. *Math. Mech. Solids* 8 (2003) 561–572.
15. C.A. Truesdell and W. Noll, In: S. Flügge (ed.), *The non-linear field theories of mechanics. Handbuch der Physik*, Vol. III/3. Heidelbrg: Springer (1965) pp. 1–602.
16. M.F. Beatty, A theory of elastic stability for incompressible hyperelastic bodies. *Int. J. Solids Struct.* 3 (1967) 23–37.
17. M.F. Beatty, Stability of the undistorted states of an isotropic elastic body. *Int. J. Nonlinear Mech.* 3 (1968) 337–349.